ORGANOMETALLICS

Article

pubs.acs.org/Organometallics

Aggregation and DNA Intercalation Properties of Di(isocyano) Rhodium(I) Diimine Complexes

Larry Tso-Lun Lo, Wing-Kin Chu, Chun-Yat Tam, Shek-Man Yiu, Chi-Chiu Ko,* and Sung-Kay Chiu*

Department of Biology and Chemistry, City University of Hong Kong, Tat Chee Avenue, Kowloon, Hong Kong SAR, People's Republic of China

Supporting Information

ABSTRACT: A series of di(isocyano) rhodium(I) diimine complexes has been synthesized and characterized. Owing to the aggregation affinity of these complexes, they were found to exhibit thermochromism. To provide further insights into the aggregation affinity of these complexes, the enthalpy (ΔH) and entropy (ΔS) changes of dimerizations of some of the complexes have been determined. In addition, the DNA intercalation properties of these complexes have also been investigated by the DNA unwinding assay.

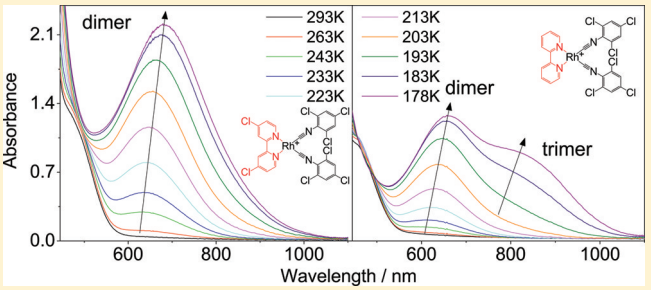

INTRODUCTION

The studies of noncovalent intermolecular interactions, such as hydrogen bonding, van der Waals force, and $\pi-\pi$, hydrophobic, and dipolar interactions, have led to the development of many different important applications.[1] Apart from these weak interactions, metal−metal interactions, in particular those of d^{10} and d^8 metal complexes with linear and square-planar geometry, were also extensively investigated.[2] The intriguing and unique photophysical properties associated with the metal−metal interactions have also been utilized for the development of sensors, light-emitting devices, and molecular wires.[3] Although the aggregation properties of square-planar Rh(I) complexes and their distinguishable photophysical properties between the monomeric and the dimeric or oligomeric species have been known for decades, many of these studies mainly focused on the binuclear systems and corresponding studies of the aggregation of mononuclear Rh(I) complexes are relatively less explored.[4]

With our interest in designing readily tunable polypyridyl isocyano metal complexes,[5] we have designed a series of di(phenylisocyano) Rh(I) diimine complexes with interesting themochromic behavior attributable to the aggregation of the mononuclear Rh(I) complex units.[6] Our preliminary results showed that the aggregation affinity of these mononuclear Rh(I) complexes could be tuned through the slight modifications of the isocyanide ligands.[6] To provide insights into the structural relationship of the thermochromic and aggregation properties, herein we report the detailed syntheses, characterization, and photophysical and aggregation properties of a new series of di(phenylisocyano) Rh(I) diimine complexes with various isocyanide and diimine ligands of diverse electronic and steric natures. As many square-planar transition metal complexes have been shown to be effective DNA intercalators,[7] which can be potentially useful for the development of antitumoral chemotherapeutic drugs, the DNA intercalation properties of these complexes have also been investigated.

Physical Measurements and Instrumentation. ^{1}H NMR spectra were recorded on a Bruker AV400 (400 MHz) FT-NMR spectrometer. Chemical shifts (δ, ppm) were reported relative to tetramethylsilane (Me_4Si). All positive-ion ESI mass spectra were recorded on a PE-SCIEX API 150 EX single quadrupole mass spectrometer. Elemental analyses of all compounds were performed on an Elementar Vario MICRO Cube elemental analyzer. Electronic absorption spectra were recorded on a Hewlett-Packard 8452A diode array spectrophotometer. The variable-temperature control was performed on an Oxford Instrument Optistat DN liquid nitrogen optical spectroscopy cryostat. Steady-state emission and excitation spectra were recorded on a Horiba Jobin Yvon Fluorolog-3-TCSPC spectrofluorometer. Measurements of the EtOH−MeOH (4:1, v/v) glass samples at 77 K were carried out with the dilute EtOH−MeOH sample solutions contained in a quartz tube inside a liquid nitrogen-filled quartz optical Dewar flask. Luminescence lifetimes of the samples were measured using the time-correlated single photon counting (TCSPC) technique on the TCSPC spectrofluorometer in a Fast MCS mode with a NanoLED-375LH excitation source, which has its excitation peak wavelength at 375 nm and pulse width shorter than 750 ps. The photon counting data were analyzed by Horiba Jobin Yvon decay analysis software.

X-ray Crystal Structure Determination. The crystal structures were determined on an Oxford Diffraction Gemini

Received: August 3, 2011
Published: October 18, 2011

S Ultra X-ray single-crystal diffractometer using graphite-monochromatized Cu-Kα radiation (λ = 1.54178 Å). The structure was solved by direct methods employing the SHELXL-97 program[8] on a PC. Rh and many non-H atoms were located according to the direct methods. The positions of other non-hydrogen atoms were found after successful refinement by full-matrix least-squares using the SHELXL-97 program[8] on a PC. In the final stage of least-squares refinement, all non-hydrogen atoms were refined anisotropically. H atoms were generated by the program SHELXL-97.[8] The positions of H atoms were calculated on the basis of the riding mode with thermal parameters equal to 1.2 times that of the associated C atoms and participated in the calculation of final *R*-indices.

DNA Unwinding Assay (ref 9). The level of DNA intercalation was determined by incubating different concentrations of the complexes from a DMSO stock solution into a pH 7.9 buffered aqueous solution containing supercoiled plasmid (pEGFP-C1, 0.5 μg), 50 mM potassium acetate, 20 mM Tris-acetate, 10 mM magnesium acetate, 1 mM dithiothreitol, and 50 μg of bovine serum albumin at 37 °C for 10 min. After the incubation, it was mixed with 2 U of *E. coli* DNA topoisomerase I for 15 min, during which supercoiling in the plasmid without any intercalator was fully and irreversibly relaxed. As DNA intercalators change the supercoiling of DNA by unwinding, only the residual supercoiling without intercalation in partially intercalated DNA would be irreversibly relaxed by the enzyme. On the contrary, there is no enzymatic relaxation in fully intercalated DNA, as no remaining supercoiling is present. Subsequently, the DNA topoisomerase reactivity was stopped by the addition of proteinase K (300 μg/mL) in 20 mM EDTA and 0.1% SDS solution to digest the DNA topoisomerase. When the intercalator was removed, the supercoiling of the intercalated portion would be reinstated. The resulting supercoiling status of the DNA, which reflects the level of DNA intercalation, was then analyzed using 0.8% agarose gel electrophoresis. The DNA bands representing the plasmid DNA with different supercoiling remaining (topoisomers) were then visualized with staining with GelRed DNA dye (Phenix Research Products, NC, USA) using an LAS-4000 luminescent image analyzer (Fujifilm Life Science).

DNA Binding: Absorption Titration Study. The base-pair concentration of CT-DNA, purchased from Calbiochem Company, was determined on the basis of the molar extinction coefficient of 6600 M^{-1} cm^{-1} at 260 nm.[10] The titration experiment was performed in a 5% DMF/5 mM Tris-HCl/50 mM NaCl buffer solution at pH 7.1 with a constant concentration of the complex and varying the CT-DNA concentrations (from 1 to 10 mol equiv). The UV−vis absorption spectra were recorded after thermal equilibration, which is about 10 min subsequent to the addition of the CT-DNA solution. The intrinsic binding constant, *K*, was determined from the linear least-squares fitting on the plot of {[CT-DNA]/($\varepsilon_a - \varepsilon_f$)} versus [CT-DNA] according to eq 1,

$$[\mathrm{CT{-}DNA}]/(\varepsilon_a - \varepsilon_f) = [\mathrm{CT{-}DNA}]/(\varepsilon_b - \varepsilon_f) + 1/[K(\varepsilon_b - \varepsilon_f)] \quad (1)$$

where [CT-DNA] is the base-pair concentration of CT-DNA, ε_a is the apparent extinction coefficient calculated from (A_{310}/[complex]), and ε_f and ε_b are the extinction coefficients for the complex in its free form and in the fully bound form at 310 nm.

SYNTHESIS AND CHARACTERIZATION

Materials and Reagents. 4,4′-Di-*tert*-butyl-2,2′-bipyridine (^{t}Bu$_2$bpy), 4,4′-dimethoxy-2,2′-bipyridine ((MeO)$_2$bpy), 4,4′-dimethyl-2,2′-bipyridine (Me$_2$bpy), 2,2′-bipyridine (bpy), 1,5-cyclooctadiene (cod), silver tetrafluoroborate ($AgBF_4$), and rhodium chloride hydrate were purchased from Strem Chemical Company and used without further purification. 4,4′-Dichloro-2,2′-bipyridine (Cl$_2$bpy) was obtained from Aldrich Chemical Co. 5,6-Diboromo-1,10-phenanthroline (Br$_2$phen) was prepared according to a previously published procedure.[11] Substituted phenyl isocyanide ligands, 4-ClC_6H_4NC, 2,4,6-$Cl_3C_6H_2$NC, 2,4,6-$Br_3C_6H_2$NC, C_6H_5NC, 2,6-^{i}Pr$_2C_6H_3$NC, and 2,6-$(CH_3)_2C_6H_3$NC, were prepared from the corresponding substituted anilines using the synthetic methodology developed by Ugi and co-workers.[12] [Rh(cod)Cl]$_2$ and rhodium(I) 1,5-cyclooctadieyl diimine complexes [Rh(bpy)(cod)]BF_4, [Rh(Me$_2$bpy)(cod)]BF_4, [Rh(Cl$_2$bpy)(cod)]BF_4, [Rh((MeO)$_2$bpy)(cod)]BF_4, [Rh(^{t}Bu$_2$bpy)(cod)]BF_4, and [Rh(Br$_2$phen)(cod)]BF_4 were synthesized according to a modified literature procedure for related complexes.[13] All solvents were of analytical reagent grade and used as received.

General Synthetic Procedure for Di(isocyano) Rhodium(I) Diimine Complexes, [Rh(CNR)$_2$(N−N)]BF_4 (1−11). To a suspension of [Rh(N−N)(cod)]BF_4 (0.5 mmol) in THF (10 mL) was added in a dropwise manner substituted phenylisocyanide (1.0 mmol) in THF (10 mL). The resulting solution was stirred at room temperature for 3 h. After removal of the solvent by rotary evaporation, the residue was washed thoroughly with copious amounts of diethyl ether to remove the displaced 1,5-cyclooctadiene and a trace amount of unreacted isocyanide ligand. Two different types of crystalline solids with red and green colors were obtained by the slow diffusion of diethyl ether vapor into a concentrated acetone, acetonitrile, or THF solution of the complexes.

1: Yield: 57%. ^{1}H NMR (400 MHz, $CDCl_3$, 298 K): δ 1.21 (d, 24H, *J* = 5.7 Hz, ^{i}Pr), 1.30−1.35 (m, 4H, ^{i}Pr), 1.42 (s, 18H, ^{t}Bu), 7.31−7.46 (m, 6H, phenyl H's), 7.74 (dd, 2H, *J* = 1.2, 5.8 Hz, 5,5′-bpy H's), 8.67 (s, br, 2H, 3,3′-bpy H's), 8.81 (d, 2H, *J* = 5.8 Hz, 6,6′-bpy H's). ESI-MS: *m*/*z* 745 [M − BF_4]$^+$. IR (KBr disk, ν/cm^{-1}): 1076 ν(B−F), 2090, 2136 ν(N≡C). Anal. Calcd for $C_{44}H_{58}N_4RhBF_4$·1/2$CHCl_3$ (found): C 59.89 (60.16), H 6.61 (6.65), N 6.28 (6.37).

2: Yield: 52%. ^{1}H NMR (400 MHz, $CDCl_3$, 298 K): δ 7.54−7.75 (m, 10H, phenyl H's), 7.77 (t, br, 2H, *J* = 6.5 Hz, 4,4′-bpy H's), 8.32 (td, 2H, *J* = 1.2, 7.8 Hz, 5,5′-bpy H's), 8.62 (d, 2H, *J* = 7.8 Hz, 3,3′-bpy H's), 8.96 (d, 2H, *J* = 6.5 Hz, 6,6′-bpy H's). ESI-MS: *m*/*z* 465 [M − BF_4]$^+$. IR (KBr disk, ν/cm^{-1}): 1084 ν(B−F), 2100, 2144 ν(N≡C). Anal. Calcd for $C_{24}H_{18}N_4RhBF_4$ (found): C 49.49 (49.77), H 3.22 (3.14), N 9.42 (9.75).

3: Yield: 59%. ^{1}H NMR (400 MHz, $CDCl_3$, 298 K): δ 7.83 (td, 2H, *J* = 1.2, 5.3 Hz, 4,4′-bpy H's), 8.04 (s, 4H, phenyl H's), 8.38 (td, 2H, *J* = 1.4, 7.9 Hz, 5,5′-bpy H's), 8.67 (d, 2H, *J* = 7.9 Hz, 3,3′-bpy H's), 9.03 (d, br, 2H, *J* = 5.3 Hz, 6,6′-bpy H's). ESI-MS: *m*/*z* 672 [M − BF_4]$^+$. IR (KBr disk, ν/cm^{-1}): 1080 ν(B−F), 2074, 2136 ν(N≡C). Anal. Calcd for $C_{24}H_{12}N_4Cl_6RhBF_4$·$CH_2Cl_2$ (found): C 35.58 (35.45), H 1.67 (1.77), N 6.64 (6.97).

4: Yield: 58%. ^{1}H NMR (400 MHz, $CDCl_3$, 298 K): δ 8.02−8.05 (m, 6H, phenyl H's and 5,5′-bpy H's), 8.96 (d, 2H, *J* = 4.1 Hz, 3,3′-bpy H's), 8.99 (d, 2H, *J* = 1.6 Hz, 6,6′-bpy H's). ESI-MS: *m*/*z* 741 [M − BF_4]$^+$. IR (KBr disk, ν/cm^{-1}): 1080 ν(B−F), 2070, 2140 ν(N≡C). Anal. Calcd for $C_{24}H_{10}N_4Cl_8RhBF_4$·1/2$H_2O$ (found): C 34.45 (34.20), H 1.33 (1.29), N 6.70 (6.58).

5: Yield: 52%. ^{1}H NMR (400 MHz, $CDCl_3$, 298 K): δ 8.06 (s, 4H, phenyl H's), 8.23 (dd, 2H, *J* = 5.1, 8.5 Hz, 3,8-phen H's), 9.08 (dd, 2H, *J* = 1.2, 8.5 Hz, 4,7-phen H's), 9.42 (d, 2H, *J* = 5.1 Hz, 2,9-phen H's). ESI-MS: *m*/*z* 854 [M − BF_4]$^+$. IR (KBr disk, ν/cm^{-1}): 1080 ν(B−F), 2080, 2146 ν(N≡C). Anal. Calcd for $C_{26}H_{10}N_4Cl_6Br_2RhBF_4$·$CH_2Cl_2$ (found): C 31.62 (31.42), H 1.18 (1.44), N 5.46 (5.51).

6: Yield: 65%. ^{1}H NMR (400 MHz, $CDCl_3$, 298 K): δ 2.49 (s, 12H, Me), 4.25 (s, 6H, OMe), 6.98 (dd, 2H, *J* = 2.6, 6.4 Hz, 5,5′-bpy H's), 7.15 - 7.27 (m, 6H, phenyl H's), 8.22 (d, 2H, *J* = 2.6 Hz, 3,3′-bpy H's), 8.50 (dd, 2H, *J* = 1.2, 6.4 Hz, 6,6′-bpy H's). ESI-MS: *m*/*z* 581 [M −

dx.doi.org/10.1021/om200723j|*Organometallics* 2011, 30, 5873−5881

Scheme 1. Synthetic Route to Di(isocyano) Rhodium(I) Diimine Complexes 1−11

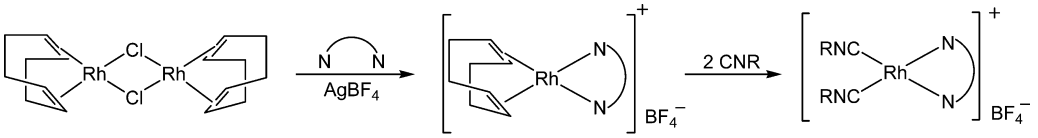

1 N-N = ^{t}Bu$_2$bpy, R = C$_6$H$_3$-(^{i}Pr)$_2$-2,6
2 N-N = bpy, R = C$_6$H$_5$
3 N-N = bpy, R = C$_6$H$_2$-Cl$_3$-2,4,6
4 N-N = Cl$_2$bpy, R = C$_6$H$_2$-Cl$_3$-2,4,6
5 N-N = Br$_2$phen, R = C$_6$H$_2$-Cl$_3$-2,4,6
6 N-N = (MeO)$_2$bpy, R = C$_6$H$_3$(CH$_3$)$_2$-2,6
7 N-N = Me$_2$bpy, R = C$_6$H$_3$(CH$_3$)$_2$-2,6
8 N-N = bpy, R = C$_6$H$_3$(CH$_3$)$_2$-2,6
9 N-N = Br$_2$phen, R = C$_6$H$_3$(CH$_3$)$_2$-2,6
10 N-N = bpy, R = C$_6$H$_4$-Cl-4
11 N-N = bpy, R = C$_6$H$_2$-Br$_3$-2,4,6

BF$_4$]$^+$. IR (KBr disk, ν/cm^{-1}): 1080 ν(B−F), 2082, 2136 ν(N≡C). Anal. Calcd for $C_{30}H_{30}N_4O_2RhBF_4$ (found): C 53.92 (53.56), H 4.52 (4.53), N 8.38 (8.61).

7: Yield: 56%. ^{1}H NMR (400 MHz, $CDCl_3$, 298 K): δ 2.49 (s, 12H, phenyl Me), 2.65 (s, 6H, bipyridyl Me), 7.15−7.24 (m, 6H, phenyl H's), 7.31 (dd, 2H, J = 1.1, 5.6 Hz, 5,5′-bpy H's), 8.57 (s, br, 2H, 3,3′-bpy H's), 8.60 (d, 2H, J = 5.6 Hz, 6,6′-bpy H's). ESI-MS: m/z 549 [M − BF$_4$]$^+$. IR (KBr disk, ν/cm^{-1}): 1080 ν(B−F), 2082, 2136 ν(N≡C). Anal. Calcd for $C_{30}H_{30}N_4RhBF_4$ (found): C 56.63 (56.67), H 4.75 (4.68), N 8.81 (9.09).

8: Yield: 54%. ^{1}H NMR (400 MHz, $CDCl_3$, 298 K): δ 2.51 (s, 12H, Me), 7.17−7.28 (m, 6H, phenyl H's), 7.59 (ddd, 2H, J = 1.2, 5.5, 8.0 Hz, 4,4′-bpy H's), 8.31 (td, 2H, J = 1.8, 5.5 Hz, 5,5′-bpy H's), 8.69 (d, 2H, J = 8.0 Hz, 3,3′-bpy H's), 8.82 (d, 2H, J = 5.5 Hz, 6,6′-bpy H's). ESI-MS: m/z 521 [M − BF$_4$]$^+$. IR (KBr disk, ν/cm^{-1}): 1080 ν(B−F), 2086, 2140 ν(N≡C). Anal. Calcd for $C_{28}H_{26}N_4RhBF_4$ (found): C 55.30 (55.67), H 4.31 (4.16), N 9.21 (9.44).

9: Yield: 48%. ^{1}H NMR (400 MHz, $CDCl_3$, 298 K): δ 2.54 (s, 12H, Me), 7.16−7.28 (m, 6H, phenyl H's), 8.24 (dd, 2H, J = 5.1, 8.6 Hz, 3,8-phen H's), 9.06 (d, 2H, J = 8.6 Hz, 4,7-phen H's), 9.27 (d, 2H, J = 5.1 Hz, 2,9-phen H's). ESI-MS: m/z 703 [M − BF$_4$]$^+$. IR (KBr disk, ν/cm^{-1}): 1080 ν(B−F), 2093, 2142 ν(N≡C). Anal. Calcd for $C_{30}H_{24}N_4Br_2RhBF_4 \cdot 1/2CH_3CN$ (found): C 45.93 (45.79), H 3.17 (2.99), N 7.78 (7.52).

10: Yield: 52%. ^{1}H NMR (400 MHz, $CDCl_3$, 298 K): δ 7.61−7.77 (m, 10H, phenyl H's and 4,4′-bpy H's), 8.32 (td, 2H, J = 1.6, 5.8 Hz, 5,5′-bpy H's), 8.60 (d, 2H, J = 8.0 Hz, 3,3′-bpy H's), 8.95 (d, 2H, J = 5.8 Hz, 6,6′-bpy H's). ESI-MS: m/z 533 [M − BF$_4$]$^+$. IR (KBr disk, ν/cm^{-1}): 1084 ν(B−F), 2097, 2144 ν(N≡C). Anal. Calcd for $C_{24}H_{16}N_4Cl_2RhBF_4 \cdot 1/2CH_3CN$ (found): C 46.80 (46.52), H 2.75 (2.72), N 9.82 (9.83).

11: Yield: 60%. ^{1}H NMR (400 MHz, $CDCl_3$, 298 K): δ 7.62 (ddd, 2H, J = 1.2, 5.6, 7.8 Hz, 4,4′-bpy H's), 7.86 (s, 4H, phenyl H's), 8.34 (td, 2H, J = 1.6, 5.6 Hz, 5,5′-bpy H's), 8.72 (d, 2H, J = 7.8 Hz, 3,3′-bpy H's), 8.94 (d, 2H, J = 5.6 Hz, 6,6′-bpy H's). ESI-MS: m/z 937 [M − BF$_4$]$^+$. IR (KBr disk, ν/cm^{-1}): 1080 ν(B−F), 2074, 2132 ν(N≡C). Anal. Calcd for $C_{24}H_{12}N_4Br_6RhBF_4 \cdot CH_3CN$ (found): C 29.28 (29.03), H 1.42 (1.66), N 6.57 (6.23).

RESULT AND DISCUSSION

Syntheses and Characterization. The synthetic route for the di(isocyano) rhodium(I) diimine complexes is summarized in Scheme 1. The precursor complexes [Rh(N−N)(cod)]BF$_4$ were synthesized by stirring the 1:1:1 mixture of [Rh(cod)Cl]$_2$, diimine ligand (N−N), and AgBF$_4$ in dichloromethane at room temperature for 2 h. Subsequent substitution reaction of these precursor complexes with 2.0 mol equiv of the substituted isocyanide ligands afforded the target di(isocyano) rhodium(I) diimine complexes **1**−**11** in moderate yields. As the diimine ligand could be further substituted on stirring with excess isocyanide ligands to give the tetra(isocyano) rhodium complex [Rh(CNR)$_4$]$^+$, thus to minimize the formation of undesirable tetra(isocyano) rhodium complex, the isocyanide ligands should be diluted in THF solution and slowly added, and an excess amount of isocyanide ligands should be avoided. Consequently, the purity of the isocyanide ligand plays an important role in the control of the yield and the purity of the crude product. Recrystallization of the crude complexes by slow diffusion of diethyl ether into concentrated solutions of **1**−**11** gave the analytically pure crystalline solids. Except complex **1**, two types of distinguishable orange-red and green crystalline solids were obtained during the recrystallization of all the complexes (Figure S1, Supporting Information). For complex **1**, only orange-red crystals were obtained on recrystallization. As demonstrated in our earlier communication,[6] the orange-red crystals were attributed to the monomeric form of the rhodium complexes, whereas the green crystals were considered to be the dimeric form of the rhodium complexes. The nonexistence of the green crystal of **1** can be explained by the significant steric repulsion between the complex monomers due to the presence of the bulky *tert*-butyl and isopropyl substituents on the diimine and the isocyanide ligands, respectively.

All complexes were characterized by ^{1}H NMR spectroscopy, IR spectroscopy, mass spectrometry, and elemental analyses. All complexes show two intense IR absorptions in the regions of 2135−2146 and 2070−2095 cm^{-1}, corresponding to the symmetric and asymmetric C≡N stretches of isocyanide ligands in a *cis*-conformation of a square-planar geometry with C_{2v} symmetry. These absorption bands are attributed to the A_1 and B_2 stretching vibrational modes.[14] For complexes with the same isocyanide ligands, the C≡N stretches follow the order **9** (2093, 2142) > **8** (2086, 2139) > **7** (2082, 2136) ≈ **6** (2082, 2136); **5** (2080, 2146) > **4** (2076, 2140) > **3** (2074, 2134), which is in the line with the π-accepting ability of the substituted diimine ligands. This trend is attributed to the competition between the isocyanides and diimine ligands for the π-back-bonding.

X-ray Crystal Structure. We have previously reported the crystal structures of both the orange-red and green crystals of complex **7**,[6] which show different intermolecular arrangements, orientations, and rhodium−rhodium metal distances. Although crystalline solids for all the complexes were obtained on recrystallization, most of them are polycrystalline or poor-quality single crystals not suitable for X-ray structure determination. The crystal structure of the red crystal of **6** shows a very similar structural arrangement to the red crystal of **7**.[6] In the red crystal of **6**, the orientations of two closest neighboring complex cation ([Rh(CNC$_6$H$_3$Me$_2$-2,6)$_2$((MeO)$_2$bpy)]$^+$) units are related by a 180° rotation with respect to the adjacent units (Figure 1). In these complex cation units, the rhodium metal center adopted a square-planar

dx.doi.org/10.1021/om200723j|*Organometallics* 2011, 30, 5873−5881

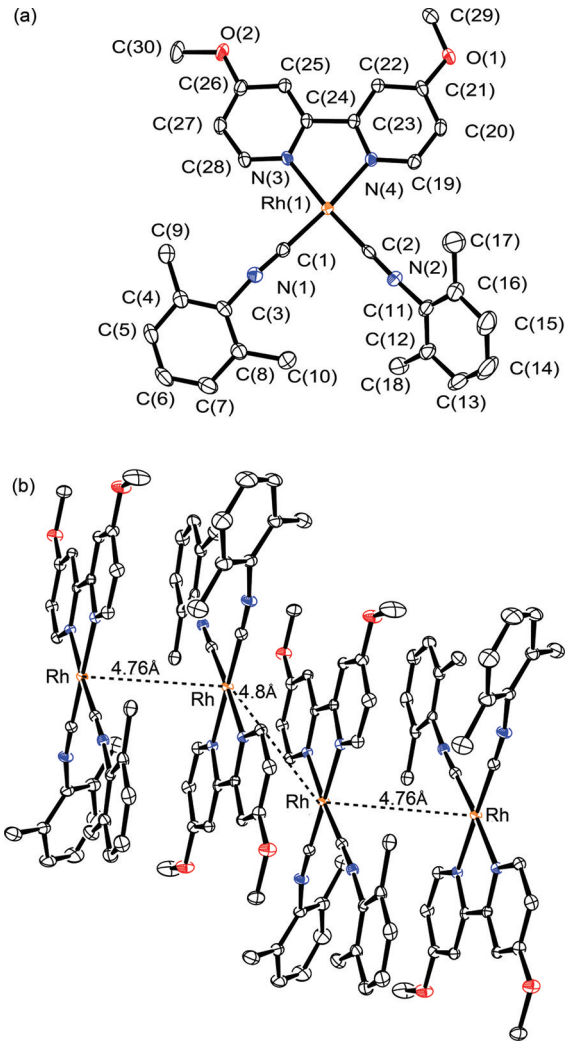

Figure 1. Ortep drawings of (a) complex cation of **6** with the atomic numbering scheme and (b) complex cations of **6** showing the intermolecular packing. Thermal ellipsoids are shown at the 50% probability level.

geometry with one coplanar isocyanide and one noncoplanar isocyanide ligand, in which the phenyl ring is tilted by 51° relative to the plane of the complexes. The shortest Rh−Rh distance between two closest complex cation molecules is ca. 4.76 Å, which is much longer than the typical Rh−Rh distances of 3.2−3.9 Å in stacked Rh(I) complexes with significant metal−metal interactions.[9] Therefore, this crystal can be considered as the monomeric form of the complex. As with other chelating diimine complexes,[10] the angle subtended by the nitrogen atoms of the bipyridine at the Rh center, N−Rh−N, was about 78.6°, which is much smaller than the ideal angle of 90° in the ideal square-planar geometry. The bending of the two isocyanide ligands as reflected from the C≡N−C bond angles of 169.0° and 173.8° can be attributed to the π-back-bonding interaction between the isocyanide ligands and the rhodium center, which is commonly observed in other metal−isocyanide complexes.[5,15]

UV−Vis Absorption and Emission Spectroscopy. Dissolution of complexes **1**−**11** in acetone and CH_2Cl_2 gave yellow to orange solutions with similar UV−vis absorption spectra (Figure S2). The electronic absorption spectra of **1**−**11** in CH_2Cl_2 show several very intense absorptions in the region of 240−330 nm, one to two moderately intense absorptions with λ_{abs} peaking at about 353−388 nm, and a weak absorption shoulder in the region of 455−490 nm (Table 3). With reference to the previous spectroscopic study of related rhodium(I) complexes,[16] the very intense absorptions are attributed to the ligand-centered (LC) $\pi \rightarrow \pi^*$ transitions of isocyanide and diimine ligands mixed with the MLCT transition [dπ(Rh) $\rightarrow$ π^*(RNC)]. For the lowest energy moderately intense absorption and weak absorption tailing in the visible region, they are ascribed to the spin-allowed and spin-forbidden MLCT [dπ(Rh) $\rightarrow$ π^*(N−N)] transitions. The

Table 1. Crystal Structure Determination Data for 6

formula	$C_{33}H_{36}BF_4N_4O_3Rh$
M_r	726.38
T/K	133(2)
a/Å	8.18060(13)
b/Å	12.82265(19)
c/Å	31.1555(4)
α/deg	90
β/deg	91.7411(13)
γ/deg	90
V/Å^3	3266.61(8)
cryst color	yellow
cryst syst	monoclinic
space group	$P2_1/c$
Z	4
F(000)	1488
D_c/g cm^3	1.477
cryst dimens/mm	0.6 × 0.1 × 0.1
λ/Å (graphite monochromated, Cu Kα)	1.541 80
absorption coeff/mm^{-1}	4.767
collection range	3.735° ≤ θ ≤ 66.98° (h: −9 to 9; k: −15 to 10; l: −37 to 37)
completeness to theta	99.9%
no. of data collected	15 093
no. of unique data	5811
no. of data used in refinement, m	5036
no. of parameters refined, p	438
R^a	0.0430
wR^a	0.0905
goodness-of-fit, S	1.101
maximum shift, $(\Delta/\sigma)_{max}$	0.001
residual extrema in final diff map, eÅ^{-3}	0.787, −0.606

$^a w = 1/[\sigma^2(F_o^2) + (ap)^2 + bP]$, where $P = [2F_c^2 + \max(F_o^2,0)]/3$.

Table 2. Selected Bond Distances (Å) and Angles (deg) with Estimated Standard Deviations (esd's) in Parentheses for 6

Bond Distances			
Rh(1)−C(1)	1.889(3)	Rh(1)−N(3)	2.076(3)
Rh(1)−C(2)	1.902(4)	Rh(1)−N(4)	2.080(3)
C(1)−N(1)	1.163(4)	C(2)−N(2)	1.168(5)
C(3)−N(1)	1.401(4)	C(11)−N(2)	1.405(5)
Bond Angles			
N(3)−Rh(1)−N(4)	78.63(10)	C(1)−Rh(1)−C(2)	88.34(14)
C(2)−Rh(1)−N(4)	96.94(12)	C(1)−Rh(1)−N(3)	96.08(12)
Rh(1)−C(1)−N(1)	177.6(3)	Rh(1)−C(2)−N(2)	178.5(3)
C(1)−N(1)−C(3)	173.8(3)	C(2)−N(2)−C(11)	169.0(4)

dx.doi.org/10.1021/om200723j|Organometallics 2011, 30, 5873−5881

Table 3. Photophysical Data for 1−11

complex	emission[a] λ_{em}/nm (τ_o/μs)	medium	T/K	absorption λ_{abs}/nm (ε/dm^3 mol^{-1}cm^{-1})
1	565 (0.47, 1.74)	CH_2Cl_2	298	244 (34145), 290 (28415), 318 sh (11585), 375 (9525), 487 (840)
		acetone	298	368 (9670), 458 (850)
		acetone	178	–[b]
2	577 (0.43, 1.53)	CH_2Cl_2	298	241 (29015), 291 (28755), 324 sh (9690), 379 (11250), 485 (1250)
		acetone	298	375 (12605), 472 (1290)
		acetone	178	705[c] (4405[d]), 903[e], 990[f]
3	568 (0.55, 2.15)	CH_2Cl_2	298	246 (25315), 302 (20435), 325 sh (10100), 370 (9230), 470 (1000)
		acetone	298	363 (11175), 453 (1010)
		acetone	178	662[c] (2960[d]), 834[e]
4	579 (0.27, 1.15)	CH_2Cl_2	298	275 (36870), 298 (36790), 382 (16490), 495 (1160)
		acetone	298	373 (17125), 485 (1070)
		acetone	178	683[c] (4990[d])
5	580 (0.54, 2.19)	CH_2Cl_2	298	249 (22410), 289 (22390), 358 (6410), 391 (5940), 496 (630)
		acetone	298	353 (14510), 380 (12825), 482 (1255)
		acetone	178	701[c] (4000[d])
6	587 (0.51, 1.43)	CH_2Cl_2	298	256 (42070), 286 (32840), 304 sh (16615), 365 (14255), 463 (1170)
		acetone	298	360 (13940), 455 (855)
		acetone	178	587[c,g]
7	574 (0.51, 1.52)	CH_2Cl_2	298	242 (31135), 290 (31050), 321 sh (9835), 374 (10975), 482 (960)
		acetone	298	369 (10760), 462 (975)
		acetone	178	626[c] (2265[d])
8	580 (0.48, 1.61)	CH_2Cl_2	298	241 (25430), 291 (25840), 323 sh (8000), 383 (8460), 488 (800)
		acetone	298	375 (10055), 475 (841)
		acetone	178	655[c,g]
9	588 (0.52, 1.74)	CH_2Cl_2	298	241 (38170), 283 (36585), 362 (7215), 401 (7860), 519 (625)
		acetone	298	362 (10200), 388 (10365), 490 (880)
		acetone	178	675[c] (1600[d])
10	570 (0.55, 1.87)	CH_2Cl_2	298	248 (19870), 295 (8545), 311 sh, (6915), 375 (4790), 483 (380)
		acetone	298	372 (11550), 470 (960)
		acetone	178	678[c,h]
11	565 (0.82, 2.30)	CH_2Cl_2	298	269 (16560), 302 (14685), 324 sh (7990), 370 (7710), 463 (675)
		acetone	298	366 (11285), 455 (850)
		acetone	178	657[c] (6275[d])

[a]Measured in EtOH−MeOH (4:1 v/v) glass at 77 K upon excitation at 400 nm. Emission maxima are uncorrected values. [b]Absorption of dimeric unit was not observed. [c]Absorption of the dimeric complexes $[Rh(CNR)_2(N{-}N)]_2^{2+}$. [d]Determined from equilibrium analysis.[4e,f,h,6] [e]Absorption of the trimeric complexes $[Rh(CNR)_2(N{-}N)]_3^{3+}$. [f]Absorption of the tetrameric complexes $[Rh(CNR)_2(N{-}N)]_4^{4+}$. [g]The absorptivity cannot be determined due to low aggregation affinity, in which the absorption of the dimeric complexes appears only at high concentration of the complex. [h]The absorptivity cannot be determined due to the precipitation of the aggregated complexes.

MLCT [dπ(Rh) → π*(N−N)] assignments are further supported by their absorption energy dependence on the electronic properties of the diimine and isocyanide ligands as revealed by the order of the absorption maxima (λ_{abs}), **3** (370, 470) < **4** (382, 495) < **5** (391, 496); **6** (365, 463) < **7** (374, 482) < **8** (383, 488) < **9** (401, 519), which is in the line with the π-accepting ability of the diimine ligand, for complexes with the same isocyanide ligand, and **3** (370, 470) ≈ **11** (370, 463) < **10** (375, 483) < **2** (379, 485) < **8** (383, 488), which is in the reverse order of the π-accepting ability of the isocyanide ligand, for the bipyridyl complexes.

As demonstrated in our previous communication,[6] the solutions of all complexes except **1** exhibit thermochromism with their color gradually changed from yellow to dark green on cooling to 178 K. The representative UV−vis absorption spectral changes of these complexes on gradual decrease of the temperature are revealed in Figure 2. For **4**−**11**, a new absorption band evolved (Figure 2a) on cooling with λ_{abs} in the range 587 to 701 nm at 178 K (Table 3). With reference to our previous study, this new absorption band is attributed to the formation of the dimeric complex $\{[Rh(CNR)_2(N{-}N)]_2\}^{2+}$

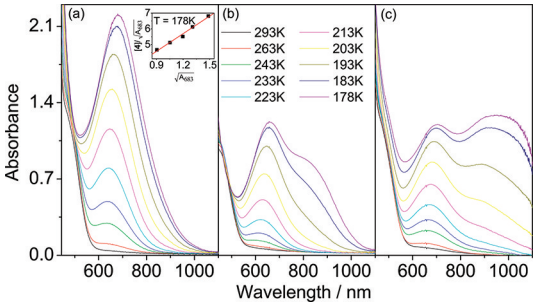

Figure 2. Overlaid UV−vis absorption spectra of the acetone solutions of (a) **4** (1.01 mM), (b) **3** (0.95 mM), and (c) **2** (0.98 mM) at different temperatures.

(Scheme 2). The dimer assignment is further validated by the linear relationship between $[Rh]_T/(A_{abs})^{1/2}$ and $(A_{abs})^{1/2}$ (Figure 2a, inset) at a constant temperature,[4e,f,h,6,17] where $[Rh]_T$ is the total concentration of the rhodium complex and A_{abs} is the absorbance at λ_{abs} of the new absorption band. Complexes **2** and **3** also show similar UV−vis absorption

dx.doi.org/10.1021/om200723j | Organometallics 2011, 30, 5873−5881

Scheme 2. Dimerization of the Rhodium(I) Complexes

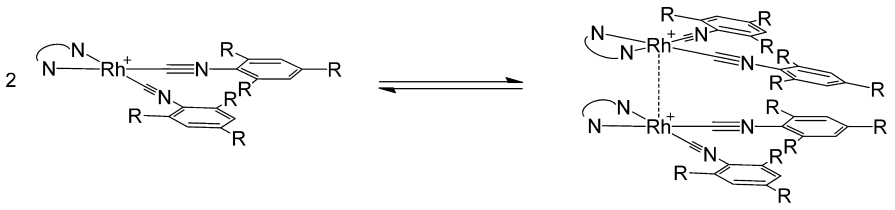

spectral changes with the evolution of one new absorption band in the same region (λ_{abs} = 705 nm for **2** and 662 nm for **3** at 178 K) at the early stage of cooling when they are in a diluted solution (<0.35 mM). In contrast, at lower temperature or in a more concentrated solution, **3** shows an additional lower energy absorption band (λ_{abs} = 834 nm at 178 K), whereas **2** shows two additional absorption bands (λ_{abs} = 903 and 990 nm at 178 K). The evolutions of the second and the third lower energy absorption bands are attributed to the formation of the trimeric and tetrameric complexes $[Rh(CNR)_2(N{-}N)]_n^{n+}$ (n = 3 and 4) as similarly observed in the tetra(isocyano) rhodium(I) complexes.[4e,f,h,16] The formation of the trimeric and tetrameric forms in **2** can be attributed to the highest aggregation affinity of **2** among **1**−**11**, as reflected by enthalpy change of dimerization (see below) due to the absence of bulky substituents on the diimine and isocyanide ligands.

Comparing the absorption of the dimeric form of the complexes with bpy (**2**, **3**, **8**, **10**, **11**) and Br_2phen (**5**, **9**) ligands, a red shift of the absorption maximum for complexes with phenylisocyanide ligands containing no substituent or less sterically bulky substituents is clearly noted, as reflected by the order of the λ_{abs} [**2** (705 nm) > **10** (678 nm) > **3** (662 nm) > **11** (657 nm) > **8** (655 nm); **5** (701 nm) > **9** (675 nm)]. These absorption maxima do not show correlation with the electronic effect of the isocyanide ligands. On the contrary, the absorption maxima of the dimeric complexes for those with identical isocyanide ligands show a clear correlation with the electronic effect of the diimine ligand and follow the order **5** (701 nm) > **4** (683 nm) > **3** (662 nm); **9** (675 nm) > **8** (655 nm) > **7** (626 nm) > **6** (587 nm), which is in line with the π-accepting ability of the diimine ligand. On the basis of these absorption energy dependences together with the previous spectroscopic work on the dinuclear rhodium complexes with bridging isocyanide ligands,[4f,j,l] these absorption bands are assigned to the transitions from $d\sigma^*[dz^2{*}(Rh)]$ to $p\sigma[pz(Rh)]$ mixed with the π^* orbital of the diimine ligand $[\pi^*(N{-}N)]$. The absorptions of the trimeric and tetrameric complexes in the lower energy region are also similarly assigned. The observation of the red-shifted absorptions of the aggregated forms for complexes with less steric bulky ligands can be explained by the shorter Rh−Rh distance and thus stronger Rh−Rh interaction in their aggregated form.[4] Similarly, the slight red shifts of the absorptions of the dimeric, trimeric, and tetrameric complexes with decreasing temperature can also be ascribed to the shortening of the Rh−Rh distance in the aggregated forms as the temperature decreased.

To provide further insights into the aggregation affinity of these complexes, the enthalpy (ΔH) and entropy (ΔS) changes of dimerizations of **2**−**5** and **11** (Table 4) are determined through the analysis of the temperature dependence of the equilibrium constants for the dimerizations using the van't Hoff equation. The ΔH of the dimerizations of these complexes range from −22.0 to −40.6 kJ mol^{-1}, which are in the same

Table 4. Summary of Thermodynamic Parameters for the Dimerization of 2−5 and 11

complex	ΔH/kJ mol^{-1}	ΔS/J mol^{-1} K^{-1}
2	−40.6	−127.4
3	−34.1	−115.9
4	−29.1	−85.3
5	−32.5	−79.7
11	−22.0	−55.5

order of magnitude for the dimerizations of related square-planar rhodium(I) and platinum(II) complexes.[4j,v,18] The negative values of all these ΔH for the dimerization reactions indicated that the dimeric form is thermodynamically more stable than the monomeric complex. On the basis of the enthalpy change of dimerization, the relative stability of the dimeric form compared to its monomeric form is found to be significantly affected by the steric properties of the isocyanide ligands as reflected by the magnitude of the enthalpy change, $|\Delta H|$, in the order of **2** (40.6) ≫ **3** (34.1) ≥ **5** (32.5) ≥ **4** (29.1) ≫ **11** (22.0). The negative entropy changes of these dimerization reactions in the range −55.5 to −127.4 J mol^{-1} K^{-1} are consistent with the decrease of the degrees of freedom of two monomeric complex molecules in the formation of the dimer. Although complexes **6**−**9** also exhibit thermochromism through the dimerization reactions, the thermodynamic parameters for these dimerization reactions were not determined since they started to show thermochromism at much lower temperature or higher concentration; thus, the van't Hoff analysis cannot be accurately performed due to the limiting data in narrow ranges of temperature and concentration.

The emission properties of these complexes were also investigated. The solids and solutions of these complexes are nonemissive at room temperature, but they become luminescent with emission maxima in the range 565−588 nm (Figure

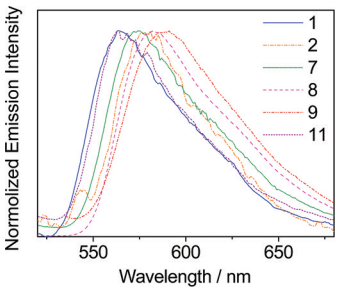

Figure 3. Overlaid normalized emission spectra of complexes **1**, **2**, **7**, **8**, **9**, and **11** in EtOH−MeOH (4:1 v/v) glass at 77 K.

3, Table 3) in EtOH−MeOH, 4:1 (v/v), glass at 77 K. Since the emissions are higher in energy compared to the absorptions of the dimeric complexes, they should be derived from the

dx.doi.org/10.1021/om200723j|*Organometallics* 2011, 30, 5873−5881

monomeric form of the complexes. In view of the relatively long-lived emission lifetimes in the submicrosecond time scale and the emission energy showing similar trends to the MLCT [$d\pi$(Rh) → π^*(N−N)] absorption bands, these emissions are tentatively assigned as derived from the ^{3}MLCT [$d\pi$(Rh) → π^*(N−N)] excited-state origin.

DNA Intercalation Study. Many important carcinogens and antitumoral chemotherapeutic drugs act on DNA by inserting themselves into the space between base pairs and unwinding the intercalated DNA. As many square-planar transition metal complexes, in particular those of platinum(II) complexes, have been shown to be effective DNA intercalators,[7] the capability of these rhodium(I) diimine complexes for DNA intercalation has also been investigated using a well-established DNA unwinding assay.[9] In this assay, plasmid DNA molecules, interacting with or without intercalator, were relaxed with DNA topoisomerase I. Subsequently, the plasmid DNA was then analyzed for their superhelicity or their range of topoisomers remaining in the population by agarose gel electrophoresis. Plasmid DNA without any intercalated molecules was fully relaxed and moved slowly in the gel (Figure 4, lane 2), while

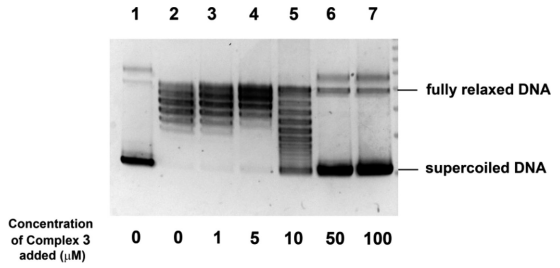

Figure 4. Complex **3** intercalated into supercoiled DNA. Supercoiled plasmid DNA was incubated with different concentrations of **3** for 10 min, then relaxed by DNA topoisomerase I and separated in agarose gel. The top of the figure is the negative electrode of the electrophoresis tank. Lane 1 contained supercoiled plasmid DNA without any treatment, which appears at the lower part of the gel. Lanes 2−7 contained plasmid DNA incubated with increasing concentration of **3** (from 0 to 100 μM). DNA topoisomers with different degrees of complex intercalation were formed and appeared as DNA bands in lane 5.

the more supercoiled or intercalated DNA molecules migrated much faster and therefore located in the lower part of the gel (Figure 4, lanes 6, 7). All complexes from 1 to 500 μM were incubated with 0.5 μg of plasmid DNA, and the remaining superhelicity of the plasmid molecules was then analyzed. Due to the low solubility of **2** and **10** and the poisoning effects of **6**−**9** on DNA topoisomerase I and proteinase K as reflected by the observation of smear located above the DNA topoisomers in the gel (Figure S3, Supporting Information), the DNA intercalation properties of these complexes cannot be determined by this assay. For other complexes, they were found to intercalate into DNA molecules with K_{int}, which is defined as the concentration of the complex at which half of the supercoiled DNA was intercalated with the complex, and display a full-range of topoisomers in agarose gel electrophoresis, ranging from 5 to 35 μM (Table S1, Supporting Information). The close resemblance of the K_{int} values (~10 μM) for **3** and **11**, which contain the same bpy ligand and different isocyanide ligands, indicated that the intercalating ability of these complexes is relatively insensitive to the changes of the isocyanide ligands and the planarity of the complexes. This is further supported by the similar intercalation ability of **1** (K_{int} ≈ 10 μM) even though it shows no intermolecular aggregation due to the steric repulsion and the nonplanarity of the complex as a result of sterically demanding 2,6-diisopropyl substituents on the isocyanide ligands. These observations suggested that the diimine ligand of the complexes is the intercalating moiety as typically reported for metal polypyridyl complexes.[19] Consequently, as Br_2phen is a more extensively conjugated intercalating ligand than bpy, **5** displayed the strongest ability in intercalation as reflected by the smallest K_{int} of less than 5 μM in this series of complexes.

The DNA intercalation of **1** to the CT-DNA was also investigated by a UV−vis absorption titration study. On addition of CT-DNA to **1** in 5% DMF/5 mM Tris-HCl/50 mM NaCl buffer solution, the absorption in the UV region, corresponding to the LC π → π^* transitions, exhibited hypochromism with a very slight red shift (ca. 2 nm) of the λ_{abs} (Figure 5). This observation is suggestive of an

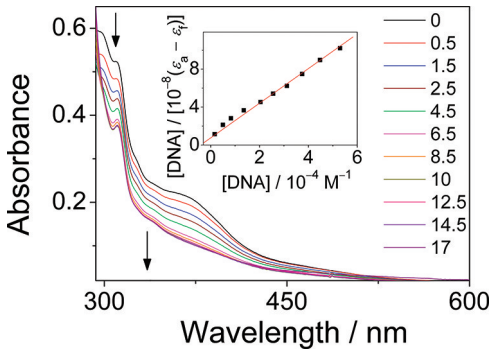

Figure 5. UV−vis absorption spectral change of **1** (30.5 μM) in a 5% DMF/5 mM Tris-HCl/50 mM NaCl buffer solution at pH 7.1 upon addition of different amounts (0, 0.5, 1.5, 2.5, 4.5, 6.5, 8.5, 10, 12.5, 14.5, and 17 mol equiv) of CT-DNA. The inset shows the plot of [CT-DNA]/($\varepsilon_{a(310)} - \varepsilon_{f(310)}$) versus [CT-DNA] and its linear least-squares fit (—).

intercalative DNA binding interaction between **1** and CT-DNA[20] and is typically observed in the DNA titration study of other intercalators.[20,21] Using the equation for CT-DNA binding and from the linear least-squares fitting of the plot of [CT-DNA] vs [CT-DNA]/($\varepsilon_a - \varepsilon_f$) (Figure 5, inset),[22] the binding constant for **1** was determined to be 2.40 × 10^4 M^{-1}, which is higher than that for other octahedral metallointercalators of tris(phenanthroline) metal complexes,[21] indicating a higher DNA intercalating affinity for these square-planar Rh(I) diimine complexes. Compared to classical organic intercalators,[23] this binding constant is similar to that of proflavine hemisulfate (2.2 × 10^4 M^{-1})[23a] but is ca. 2 orders of magnitude lower than that for ethidium bromide (1.25 × 10^6 M^{-1})[23b,c] under similar experimental conditions. This trend is consistent with the results found in the DNA unwinding assay.

CONCLUSION

A new series of thermochromic di(isocyano) rhodium(I) diimine complexes, [Rh(CNR)$_2$(N−N)]$^+$, with different isocyanide and diimine ligands has been successfully synthesized and characterized, and their photophysical and thermochromic properties have been studied. The detailed study revealed that the thermochromic properties of these complexes can be significantly modified through the change of

dx.doi.org/10.1021/om200723j | Organometallics 2011, 30, 5873−5881

the substituents of the isocyanide ligands. To provide insights into the aggregation affinity and the future design of thermally responsive molecular devices based on the square-planar rhodium(I) complexes, the enthalpy (ΔH) and entropy (ΔS) changes of the dimerizations of some of the complexes have been determined. In addition, the DNA intercalation properties of these rhodium(I) complexes have also been investigated by the DNA unwinding assay, which showed that these complexes can intercalate DNA at micromolar range. Further modifications of the diimine ligands on these complexes to enhance their DNA intercalation ability and the study of their potential applications as antitumoral chemotherapeutic drugs are now in progress.

■ ASSOCIATED CONTENT

Ⓢ Supporting Information

CIF files giving crystal data of **6**, photographs showing two different types of crystals obtained during the course of recrystallization, overlaid UV−vis spectra of selected complexes, and table summarizing the K_{int} in the DNA intercalation study. This material is available free of charge via the Internet at http://pubs.acs.org.

■ AUTHOR INFORMATION

Corresponding Author

*E-mail: vinccko@cityu.edu.hk; kaychiu@cityu.edu.hk. Fax: (+852)-3442-0522. Tel: (+852)-3442-6958.

■ ACKNOWLEDGMENTS

The work described in this paper was supported by a RGC GRF grant from the Research Grants Council of Hong Kong (Project No. CityU 101510) and a grant from City University of Hong Kong (Project No. 7002688). L.T.-L.L. and W.-K.C. acknowledge the receipt of a Postgraduate Studentship and a Research Tuition Scholarship, both administrated by City University of Hong Kong.

■ REFERENCES

(1) (a) Lehn, J.-M. *Angew. Chem., Int. Ed. Engl.* **1988**, *27*, 90. (b) Philp, D.; Stoddart, J. F. *Angew. Chem., Int. Ed. Engl.* **1996**, *35*, 90. (c) Cram, D. J.; Cram, J. M. *Acc. Chem. Res.* **1978**, *11*, 7. (d) Hoss, R.; Vögtle, F. *Angew. Chem., Int. Ed. Engl.* **1994**, *33*, 375.

(2) (a) Jenette, K. W.; Gill, J. T.; Sadownick, J. A.; Lippard, S. J. *J. Am. Chem. Soc.* **1976**, 6159. (b) Balch, A. L. In *Extended Linear Chain Compounds*, Vol. *1*; Plenum: New York, 1982. (c) *Chemistry and Physics of One-Dimensional Metals*; Keller, H. J., Ed.; Plenum Press: New York. (d) *Extended Linear Chain Compounds*; Miller, J. S., Ed.; Plenum: New York, 1982. (e) Vogler, A.; Kunkely, H. *Chem. Phys. Lett.* **1988**, *150*, 135. (f) Pyykko, P.; Zhao, Y. *Angew. Chem., Int. Ed. Engl.* **1991**, *30*, 604. (g) Schmidbaur, H. *Chem. Soc. Rev.* **1995**, 391. (h) Yam, V. W.-W.; Cheng, E. C.-C. *Top. Curr. Chem.* **2007**, *281*, 269. (i) Phillips, D. L.; Che, C.-M.; Leung, K.-H.; Zhong, M.; Tse, M.-C. *Coord. Chem. Rev.* **2005**, *249*, 1476. (j) Williams, J. A. G. *Top. Curr. Chem.* **2007**, *281*, 205. (k) Bera, J. K.; Dunbar, K. R. *Angew. Chem., Int. Ed.* **2002**, *41*, 4453. (l) Tejel, C.; Ciriano, M. A.; Oro, L. A. *Chem.—Eur. J.* **1999**, *5*, 1131. (m) Houlding, V. H.; Miskowski, V. M. *Coord. Chem. Rev.* **1991**, 145. (n) Yajima, T.; Maccarrone, G.; Takani, M.; Contino, A.; Arena, G.; Takamido, R.; Hanaki, M.; Funahashi, Y.; Odani, A.; Yamauchi, O. *Chem.—Eur. J.* **2003**, 3341. (o) Connick, W. B.; Henling, L. M.; Marsh, R. E.; Gray, H. B. *Inorg. Chem.* **1996**, 6261. (p) Hill, M. G.; Bailey, J. A.; Miskowski, V. M.; Gray, H. B. *Inorg. Chem.* **1996**, 4685.

(3) (a) Exstrom, C. L.; Sowa, J. R. Jr.; Daws, C. A.; Janzen, D.; Mann, K. R.; Moore, G. A.; Stewart, F. F. *Chem. Mater.* **1995**, *7*, 15. (b) Tang, W.-S.; Lu, X.-X.; Wong, K. M.-C.; Yam, V. W.-W. *J. Mater Chem.* **2005**, *15*, 2714. (c) Yam, V. W.-W.; Lu, X.-X.; Ko, C.-C. *Angew. Chem., Int. Ed.* **2003**, *42*, 3385. (d) Yam, V. W.-W.; Tang, R. P.-L.; Wong, K. M.-C.; Ko, C.-C.; Cheung, K.-K. *Inorg. Chem.* **2001**, *40*, 571.

(4) (a) Balch, A. L. *J. Am. Chem. Soc.* **1976**, *98*, 8049. (b) Shafiq, F.; Kramarz, K. W.; Eisenberg, R. *Inorg. Chem. Acta* **1993**, *213*, 111. (c) Braunschweig, H.; Forster, M.; Radacki, K. *Angew. Chem., Int. Ed.* **2006**, *45*, 2132. (d) Bo, C.; Costas, M.; Poblet, J. M.; Rohmer, M.-M.; Benard, M. *Inorg. Chem.* **1996**, *35*, 3298. (e) Mann, K. R.; Gordon, J. G. II; Gray, H. B. *J. Am. Chem. Soc.* **1975**, *97*, 3553. (f) Lewis, N. S.; Mann, K. R.; Gordon, J. G. II; Gray, H. B. *J. Am. Chem. Soc.* **1976**, *98*, 7461. (g) Dart, J. W.; Lloyd, M. K.; Mason, R.; McCleverty, J. A. *J. Chem. Soc., Dalton Trans.* **1973**, 2039. (h) Mann, K. R.; Lewis, N. S.; Williams, R. M.; Gray, H. B. *Inorg. Chem.* **1978**, *17*, 828. (i) Miskowski, V. M.; Sigal, I. S.; Mann, K. R.; Gray, H. B. *J. Am. Chem. Soc.* **1979**, *101*, 4383. (j) Rice, S. F.; Gray, H. B. *J. Am. Chem. Soc.* **1981**, *103*, 1593. (k) Fordyce, W. A.; Brummer, J. G.; Crosby, G. A. *J. Am. Chem. Soc.* **1981**, *103*, 7061. (l) Miskowski, V. M.; Rice, S. F.; Gray, H. B.; Milder, S. J. *J. Phys. Chem.* **1993**, *97*, 4277. (m) Fortin, D.; Drouin, M.; Harvey, P. D. *J. Am. Chem. Soc.* **1997**, *119*, 531. (n) Tejel, C.; Ciriano, M. A.; Lopez, J. A.; Lahoz, F. J.; Oro, L. A. *Angew. Chem., Int. Ed.* **1998**, *37*, 1542. (o) Tejel, C.; Ciriano, M. A.; Oro, L. A. *Chem.—Eur. J.* **1999**, *5*, 1131. (p) Heyduk, A. F.; Macintosh, A. M.; Nocera, D. G. *J. Am. Chem. Soc.* **1999**, *121*, 5023. (q) Bradley, P. M.; Bursten, B. E.; Turro, C. *Inorg. Chem.* **2001**, *40*, 1376. (r) Bera, J. K.; Dunbar, K. R. *Angew. Chem., Int. Ed.* **2002**, *41*, 4453. (s) Cooke, M. W.; Hanan, G. S.; Loiseau, F.; Campagna, S.; Watanabe, M.; Tanaka, Y. *Angew. Chem., Int. Ed.* **2005**, *44*, 4881. (t) Tran, N. T.; Stork, J. R.; Pham, D.; Chancellor, C. J.; Olmstead, M. M.; Fettinger, J. C.; Balch, A. L. *Inorg. Chem.* **2007**, *46*, 7998. (u) Tran, N. T.; Stork, J. R.; Pham, D.; Olmstead, M. M.; Fettinger, J. C.; Balch, A. L. *Chem. Commun.* **2006**, 1130. (v) Grimme, S.; Djukic, J.-P. *Inorg. Chem.* **2011**, *50*, 2619.

(5) (a) Cheung, A. W.-Y.; Lo, L. T.-L.; Ko, C.-C.; Yiu, S.-M. *Inorg. Chem.* **2011**, *50*, 4798. (b) Ko, C.-C.; Siu, J. W.-K.; Cheung, A. W.-Y.; Yiu, S.-M. *Organometallics* **2011**, *30*, 2701. (c) Ko, C.-C.; Lo, L. T-L.; Ng, C.-O.; Yiu, S.-M. *Chem.—Eur. J.* **2010**, 13773. (d) Ng, C.-O.; Lo, L. T.-L.; Ng, S.-M.; Ko, C.-C.; Zhu, N. *Inorg. Chem.* **2008**, *48*, 7447.

(6) Lo, L. T.-L.; Ng, C.-O.; Feng, H.; Ko, C.-C. *Organometallics* **2009**, *29*, 3597.

(7) Liu, H.-K.; Sadler, P.-J. *Acc. Chem. Res.* **2011**, *44*, 349.

(8) Sheldrick, G. M. *SHELX-97: Programs for Crystal Structure Analysis* (Release 97-2); University of Goettingen: Germany, 1997.

(9) (a) Shen, L. L. *DNA Topoisomerase Protocols* Bjornsti, M.-A.; Osheroff, N., Eds.; 1999; Vol. *94*, pp 149−160. (b) Peixoto, P.; Bailly, C.; David-Cordonnier, M. H. *Methods Mol. Biol.* **2010**, *613*, 235.

(10) Reichmann, M. E.; Rice, S. A.; Thomas, C. A.; Doty, P. *J. Am. Chem. Soc.* **1954**, *76*, 3047.

(11) Mlochowski, J. *J. Rocz. Chem.* **1974**, *48*, 2145.

(12) (a) Ugi, I.; Fetzer, U.; Eholzer, U.; Knupfer, H.; Offermann, K. *Angew. Chem., Int. Ed. Engl.* **1965**, *4*, 472. (b) Obrecht, R.; Herrmann, R.; Ugi, I. *Synthesis* **1985**, *4*, 400.

(13) Ribeiro, E. A.; Donnici, C. L.; Santos, E. N. dos. *J. Organomet. Chem.* **2006**, *691*, 2037. (b) Mestroni, G.; Camus, A.; Zassinovich, G. *J. Organomet. Chem.* **1974**, *73*, 119.

(14) Adams, D. M.; Trumble, W. R. *Dalton Trans.* **1974**, *7*, 690.

(15) Weber, L. *Angew. Chem., Int. Ed.* **1998**, *37*, 1515.

(16) (a) Rice, S. F.; Milder, S. J.; Gray, H. B.; Goldbeck, R. A.; Kliger, D. S. *Coord. Chem. Rev.* **1982**, *43*, 349. (b) Yamamoto, Y.; Wakatsuki, Y.; Yamazaki, H. *Organometallics* **1983**, *2*, 1604. (c) Oppelt, K.; Egbe, D. A. M.; Monkowius, U.; List, M.; Zabel, M.; Sariciftci, N. S.; Knör, G. *J. Organomet. Chem.* **2011**, *696*, 2052.

(17) Miya, S.; Yamamoto, Y.; Yamazaki, H. *Inorg. Chem.* **1982**, *21*, 1486.

(18) (a) Novoa, J. J.; Aullon, G.; Alemany, P.; Alvarez, S. *J. Am. Chem. Soc.* **1995**, 7169. (b) Sakaki, S.; Ogawa, M.; Musashi, Y. *J. Phys. Chem.* **1995**, *99*, 17134. (c) Sugimoto, M.; Horiuchi, F.; Sakaki, S. *Chem. Phys. Lett.* **1997**, *274*, 543.

(19) (a) Jain, A.; Wang, J.; Mashack, E. R.; Winkel, B. S. J.; Brewer, K. J. *Inorg. Chem.* **2009**, *48*, 9077. (b) Petitjean, A.; Barton, J. K. *J. Am. Chem. Soc.* **2004**, *126*, 14728. (c) Wheatea, N. J.; Brodiea, C. R.;

Collinsb, J. G.; Kempa, S.; Aldrich-Wrighta, J. R. *Mini-Rev. Med. Chem.* **2007**, *7*, 627. (d) Zeglis, B. M.; Pierre, V. C.; Kaiser, J. T.; Barton, J. K. *Biochemistry* **2009**, *48*, 4247. (e) Xu, Z.; Swavey, S. *Dalton Trans.* **2011**, *40*, 7319. (f) Choudhury, J. R.; Rao, L.; Bierbach, U. *J. Biol. Inorg. Chem.* **2011**, *16*, 373.

(20) Long, E. C.; Barton, J. K. *Acc. Chem. Res.* **1990**, *23*, 271.

(21) (a) Morgan, R. J.; Chatterjee, S.; Baker, A. D.; Strekas, T. C. *Inorg. Chem.* **1991**, *30*, 2687. (b) Ramakrishnan, S.; Palaniandavar, M. *Dalton Trans.* **2008**, 3866. (c) Talib, J.; Harman, D. G.; Dillon, C. T.; Aldrich-Wright, J.; Beck, J. L.; Ralpg, S. F. *Dalton Trans.* **2009**, 504. (d) Ramakrishnan, S.; Suresh, E.; Riyasdeem, A.; Akbarsha, M. A.; Palaniandavar, M. *Dalton Trans.* **2011**, 3524.

(22) (a) Meehan, T.; Gamper, H.; Becker, J. F. *J. Biol. Chem.* **1982**, 10479. (b) Wolfe, A.; Shimer, G. H. Jr.; Meehan, T. *Biochemistry* **1987**, 6392.

(23) (a) Aslanoglu, M. *Anal. Sci.* **2006**, 439. (b) Tang, T.-C.; Huang, H.-J. *Electroanalysis* **1999**, *11*, 1185. (c) Burya, S. J.; Lutterman, D. A.; Turro, C. *Chem. Commun.* **2011**, *47*, 1848.